Stable dispersions of poly(ethylene glycol) methyl ether-magnetite complexes in water

Thapanapong Theppaleak[a]; Uthai Wichai[a]; Boonjira Boontha[a]; Gamolwan Tumcharern[b]; Metha Rutnakornpituk[a]

[a] Department of Chemistry and Centre of Excellence for Innovation in Chemistry, Naresuan University, Phitsanulok, Thailand [b] National Nanotechnology Centre, National Science and Technology Development Agency, Pathumthani, Thailand

PLEASE SCROLL DOWN FOR ARTICLE

Taylor & Francis
Taylor & Francis Group

Stable dispersions of poly(ethylene glycol) methyl ether–magnetite complexes in water

Thapanapong Theppaleak[a], Uthai Wichai[a], Boonjira Boontha[a], Gamolwan Tumcharern[b] and Metha Rutnakornpituk[a]*

[a]*Department of Chemistry and Centre of Excellence for Innovation in Chemistry, Naresuan University, Phitsanulok, Thailand;* [b]*National Nanotechnology Centre, National Science and Technology Development Agency, Pathumthani, Thailand*

We herein describe a facile synthesis of superparamagnetic magnetite ferrofluids having long-term stability in aqueous dispersions. A single-step thermal decomposition reaction of iron (III) acetylacetonate ($Fe(acac)_3$) was carried out in the presence of poly(ethylene glycol) methyl ether (mPEG) to serve both as a reducing agent and reaction solvent. The role of number average molecular weight ($\overline{M}_n$) of mPEG (350 and 750 g/mol) on the size and properties of the particles was investigated. Fourier-transform infrared spectrophotometry (FTIR) indicated the presence of mPEG in the polymer–magnetite complexes. According to thermogravimetric analysis (TGA), the complexes consisted of 40–66% Fe_3O_4, depending on the molecular weights of mPEG used. According to the transmission electron micrographs (TEM), the particles prepared in 350 g/mol mPEG exhibited the average diameter of 7.8 ± 1.4 nm, while those in 750 g/mol mPEG were 5.3 ± 1.1 nm. From photocorrelation spectroscopy (PCS) experiments, the size of 350 g/mol mPEG–magnetite complex and 750 g/mol mPEG–magnetite complex were 37.1 ± 1.0 nm and 35.1 ± 0.4 nm, respectively. According to the calculation by the Debye–Scherrer equation, the sizes of 350 g/mol mPEG–magnetite complex and 750 g/mol mPEG–magnetite complex were 7.7 and 6.6 nm, respectively. They were highly crystalline and exhibited superparamagnetic properties. They were stable in aqueous dispersions with insignificant aggregation after 6 weeks of preparing. These stable, non-toxic dispersions might be potentially used in magnetically targeted biomedical applications.

Keywords: magnetite; nanoparticle; poly(ethylene glycol) methyl ether; water dispersible

1. Introduction

Magnetite ferrofluids have recently attracted marked attention for uses in many biomedical applications such as hyperthermia [1–4], magnetic resonance imaging (MRI) [5–12] and magnetic drug targeting [13–17]. They have been known as biocompatible,

*Corresponding author. Email: methar@nu.ac.th

non-toxic and chemical-resistant materials. However, magnetite nanoparticles in ferrofluids tend to agglomerate to each other due to van der Waals and magnetic attractive forces. Hence, the studies in preventing aggregation of these nanoparticles have been greatly focussed. Many recent studies have reported the synthesis of water dispersible magnetite nanoparticles through one-pot decomposition of iron (III) acetylacetonate (Fe(acac)$_3$) in merely organic compounds containing hydroxyl groups, such as benzyl alcohol [18], tetraethylene glycol and triethylene glycol [19]. These compounds functioned as both reaction solvents and reducing agents because they have high boiling points, high polarities and OH reactive functional groups. Although water dispersible magnetite nanoparticles were obtained, long-term stability in aqueous medium is concerned if they are anticipated for uses in biomedical applications due to a lack of long-chain polymeric surfactants on the particle surfaces. Li et al. [20] have reported the synthesis of magnetite nanoparticles in 2-pyrolidone using dicarboxyl-terminated poly(ethyelene glycol) as surfactants. They proposed that carboxylic acid can coordinate on the particle surfaces. However, stability of the dispersions in water for a long period of time was not reported.

In this study, we used poly(ethylene glycol) methyl ether (mPEG) oligomers as both reducing agent and reaction solvent in the thermal decomposition reaction of Fe(acac)$_3$. Hydroxyl groups at mPEG chain termini are thought to coordinate onto the particle surface [18,19,21–24] and poly(ethylene glycol) chains provide steric stabilisation and dispersibility in water. This is the first study on preparing magnetite nanoparticles via organic solvent-free thermal decomposition in the presence of merely hydrophilic oligomers having OH groups in the reactions. Two different number average molecular weights ($\overline{M}_n$) of mPEG (350 and 750 g/mol) were used in this study to investigate the effect of their chain length on the structure and magnetic properties of the as-synthesised complexes. Fourier-transform infrared spectrophotometry (FTIR) was used to evidence the presence of mPEG in the complexes. Their structure was elucidated using X-ray diffractometry (XRD), and their particle size was investigated using transmission electron microscopy (TEM) and photocorrelation spectroscopy (PCS). Their magnetic properties were investigated via vibrating sample magnetometry (VSM). Their long-term stability in water and cytotoxicity testing were also performed to study the feasibility for use in biomedical applications.

2. Experimental procedure

2.1. *Materials*

The mPEG with $\overline{M}_n$ 350 g/mol and 750 g/mol (Acros) were freeze-dried prior to use and Fe(acac)$_3$, 99+% (Acros), was used as received. Cellulose dialysis tubing (Sigma–Aldrich) with molecular weight cut off (MWCO) 12,400 was immersed in running water for 24 h before being used.

2.2. *Characterisation*

FTIR was performed on a Perkin Elmer Model 1600 series FTIR spectrophotometer. Magnetite concentrations in dispersions were analysed by flame atomic absorption spectrometer (AAS). XRD patterns of the particles were collected on a Philips X'pert

X-ray diffractometer under Cu-Kα radiation ($\lambda = 1.540598\,\text{Å}$) operated at $30\,\text{kV}$ and 2θ ranging from $0°$ to $90°$. The particle size was estimated form XRD patterns following the Debye–Scherrer equation [25–27], $D = 0.9\lambda/\beta\cos\theta$, where D is the average crystallite size (Å), λ is the wavelength of X-rays (Cu-Kα; $\lambda = 1.540598\,\text{Å}$), θ is the Bragg diffraction angle and β is the full width at half maximum (FWHM). For TEM analyses, samples were dried on carbon-coated copper grids and the images were taken using a Philips Tecnai 12 operated at $120\,\text{kV}$ equipped with Gatan model 782 CCD camera. Hydrodynamic diameter of the particles was measured at $25°C$ via PCS using NanoZS4700 nanoseries Malvern instrument. The sample dispersions were sonicated for $10\,\text{min}$ before each measurement. Magnetic properties were measured at $300\,\text{K}$ using a standard 7403 series, Lakeshore VSM. The magnetic moment of each sample was investigated over a range of applied magnetic fields from $-10,000$ to $+10,000\,\text{G}$ using $30\,\text{min}$ sweep time. Mass specific magnetisations were calculated using the concentration of iron measured by AAS and assuming that all irons were in the form of magnetite. Thermogravimetric analysis (TGA) was performed on SDTA 851 Mettler-Toledo at temperatures ranging between $25°C$ and $600°C$ at a heating rate of $20°C/\text{min}$ under oxygen atmosphere. It is assumed that all organic components were thermally decomposed and iron oxide remained as char.

2.3. *Synthesis of water-dispersible mPEG–magnetite complexes*

Fe(acac)$_3$ ($0.5\,\text{g}$, $0.0014\,\text{mole}$) was mixed with mPEG ($20\,\text{ml}$) in three-neck round-bottom flask equipped with a mechanical stirrer. The reaction was heated to $200°C$ for $6\,\text{h}$ under N$_2$ blanket. After cooling, the dispersions were centrifuged at $5000\,\text{rpm}$ to precipitate some aggregate. The dispersions were then dialysed against water and refreshed twice every $24\,\text{h}$ interval to remove uncoordinated species, followed by centrifugation to again remove some aggregate. These dispersions were used for TEM and PCS analyses. The samples for FTIR, VSM and XRD were prepared by a freeze-drying technique from the aqueous dispersions to obtain solid samples of mPEG–magnetite complexes.

3. Results and discussion

The main aim of this study is to develop a facile single-step synthesis of magnetite nanoparticles having long-term stability in aqueous dispersions. Precedents have reported a single-pot thermal decomposition of Fe(acac)$_3$ in the presence of small organic molecules containing reactive functional groups [18,19]. However, long-term stability of the as-prepared dispersions in water is concerned for uses in biomedical applications. In an attempt to extend the stability of the particles in water, we have recently reported a one-step reaction to obtain water dispersible magnetite nanoparticles by the thermal decomposition of Fe(acac)$_3$ in other reducing systems [28]. The reaction was carried out in the presence of water soluble carboxylic acid-terminated mPEG acid, poly(vinyl alcohol) (PVA) and NH$_2$-containing polyether (Jefamine M-2070). The as-synthesised particles were stable in water over one-month period without any significant aggregation observed. In addition, our interest is also extended to investigate the effect of polymer functional groups on the particle stability in the dispersions; thermal decomposition reactions of Fe(acac)$_3$ solely in carboxylic acid-, amine- or hydroxyl-containing water-soluble polymers are systematically performed. In this study, we primarily aimed at facilitating the synthesis

of water dispersible magnetite nanoparticles by using merely hydrophilic mPEG oligomers in the thermal decomposition reaction of Fe(acac)$_3$ and also extended their stability in aqueous dispersions.

FTIR spectra of the as-synthesised particles were exhibited to compare with those of the iron precursor and mPEG oligomers (Figure 1). Both mPEG–magnetite complex spectra showed a strong signal at ~588 cm^{-1}, which is the characteristic signal of Fe–O bonds of magnetite. Besides, the signals at ~1102 cm^{-1} corresponding to C–O stretching and at 3418–3369 cm^{-1} corresponding to O–H stretching indicated the presence of mPEG in the complexes. It should be noted once again that an excess mPEG was removed from the dispersions using dialysis technique. In addition, it is noteworthy that ratio of the peak area of C–O bonds (~1103 cm^{-1}) to Fe–O bonds (~588 cm^{-1}) of 750 g/mol mPEG–magnetite complex (spectrum (d) in Figure 1) was higher than that of 350 g/mol mPEG–magnetite complex (spectrum (c) in Figure 1), implying that 750 g/mol mPEG–magnetite complex possessed more mPEG in its composition. In other words, 350 g/mol mPEG–magnetite complex might contain higher content of Fe$_3$O$_4$ in its composition.

Percent weight loss of these complexes was determined via TGA technique to estimate the percent of magnetite in the complex, which reflect the amount of mPEG oligomer
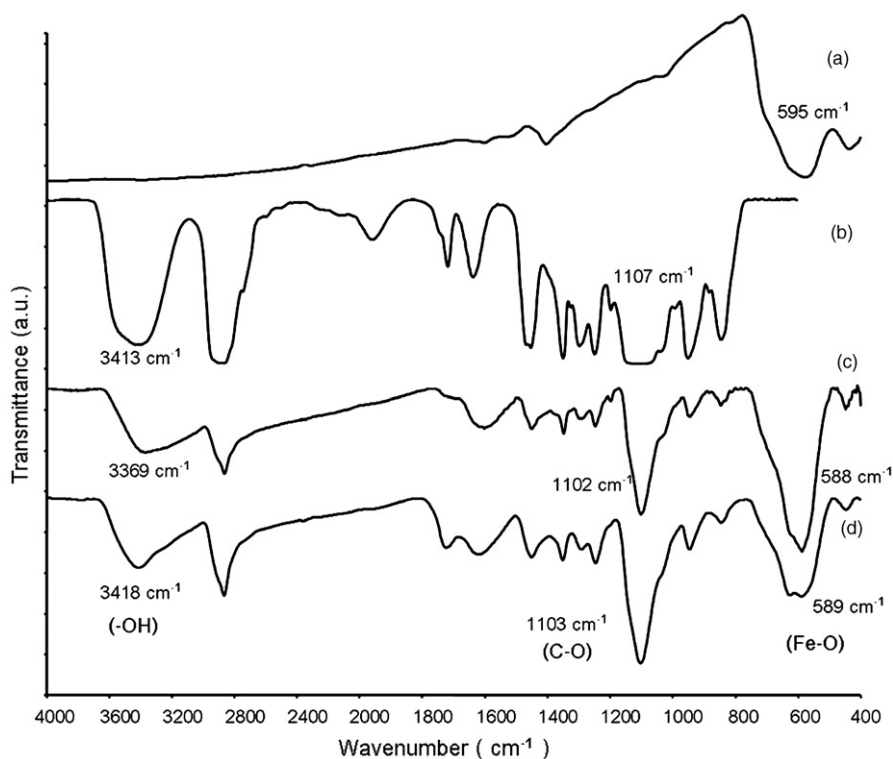

Figure 1. FTIR spectra of (a) bare Fe$_3$O$_4$, (b) 750 g/mol mPEG oligomers, (c) 350 g/mol mPEG–magnetite complex and (d) 750 g/mol mPEG–magnetite complex.

in their composition. It was assumed that the percentage yield of char is the weight percent of iron oxide in the form of magnetite that remained after the decomposition of mPEG oligomer at 600°C and the percentage of weight loss is the weight percent of mPEG in the complex. The result showed about 66% Fe_3O_4 in 350 g/mol mPEG–magnetite complexes (34% polymer) and only 40% Fe_3O_4 in 750 g/mol mPEG–magnetite complex (60% polymer) (Figure 2). It was rationalised that relatively high molecular weight of mPEG (750 g/mol) might provide a thick polymeric surfactant layer on the particle surface with OH groups coordinating on their surface [18,19,21–24]. This result was in good agreement with those observed by FTIR, indicating higher percent of the polymers in 750 g/mol mPEG–magnetite complex than the other one.

According to the TEM images and particle size distributions in Figure 3((a)–(d)), the size of 350 g/mol mPEG–magnetite complex was ranging between 5 and 10 nm in diameter with the average size of 7.8 ± 1.4 nm, while the size of 750 g/mol mPEG–magnetite complex was ranging between 3 and 10 nm in diameter with the average size of 5.3 ± 1.1 nm.

A PCS technique was performed to determine the hydrodynamic diameter of the as-synthesised particles in aqueous dispersions. The sizes of 350 g/mol mPEG–magnetite complex and 750 g/mol mPEG–magnetite complex were 37.1 ± 1.0 nm and 35.1 ± 0.4 nm, respectively (Figure 4). The sizes were significantly larger than those observed from TEM technique probably because the particles occupied large volume of water due to the presence of hydrophilic mPEG in the complex in combination with the presence of some nanoscale agglomeration of multiple nanoparticles in water. In addition, there was some large particle cluster of the 750 g/mol mPEG–magnetite complex observed in the PCS size distribution histogram (size ~60–600 nm; Figure 4(b)). This phenomenon arose probably owing to the entanglement of relatively long hydrophilic chain length of 750 g/mol mPEG compared to those of 350 g/mol mPEG, which might influence the particle formation and their dispersibility during the thermal decomposition reaction.

From XRD studies, the position and relative intensities of all diffraction signals matched well with the characteristic peaks of magnetite crystal [29] ($2\theta = 30.2°$, $35.6°$,
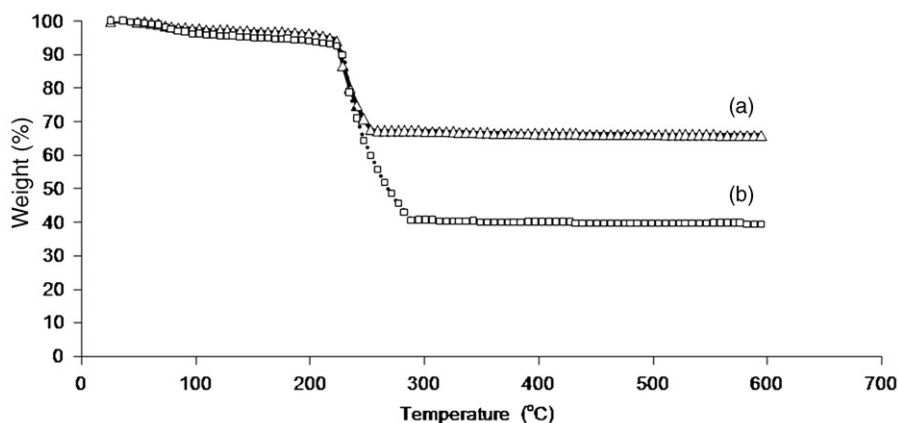

Figure 2. TGA thermograms of (a) 350 g/mol mPEG–magnetite complex and (b) 750 g/(mol mPEG–magnetite complex.
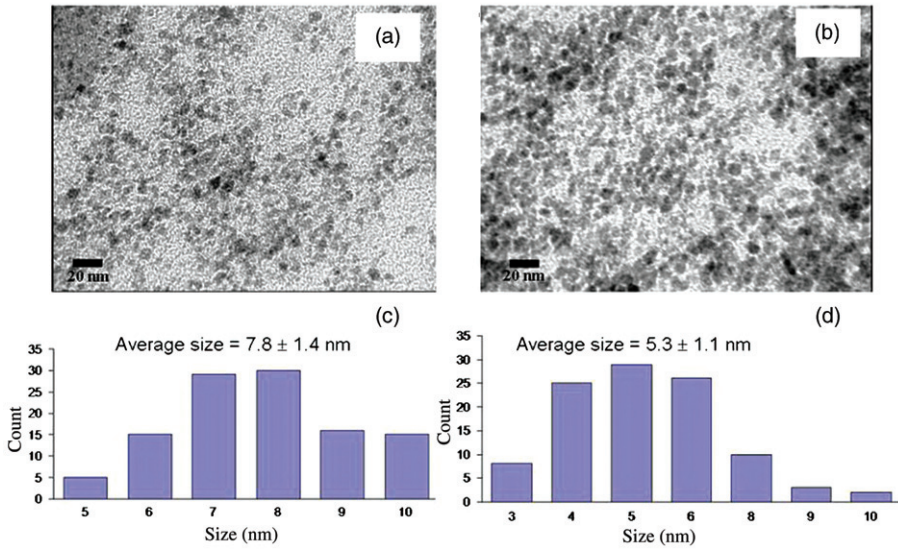
Figure 3. (A) a TEM image, (B) a TEM image, (C) particle size distribution of 350 g/mol mPEG–magnetite complex and (D) particle size distribution of 750 g/mol mPEG–magnetite complex.
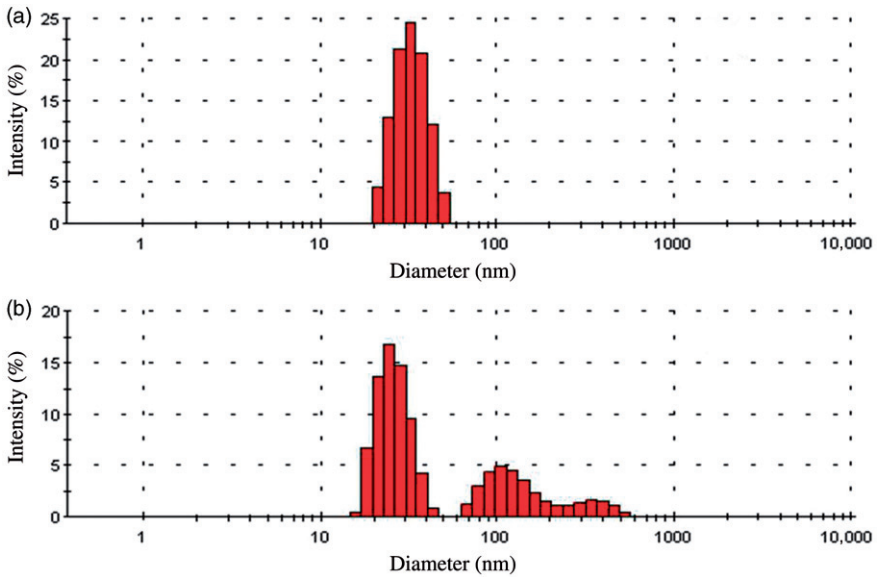Note: These samples were directly cast from aqueous dispersions.

Figure 4. PCS size distributions of (a) 350 g/mol mPEG–magnetite complex and (b) 750 g/mol mPEG–magnetite complex.
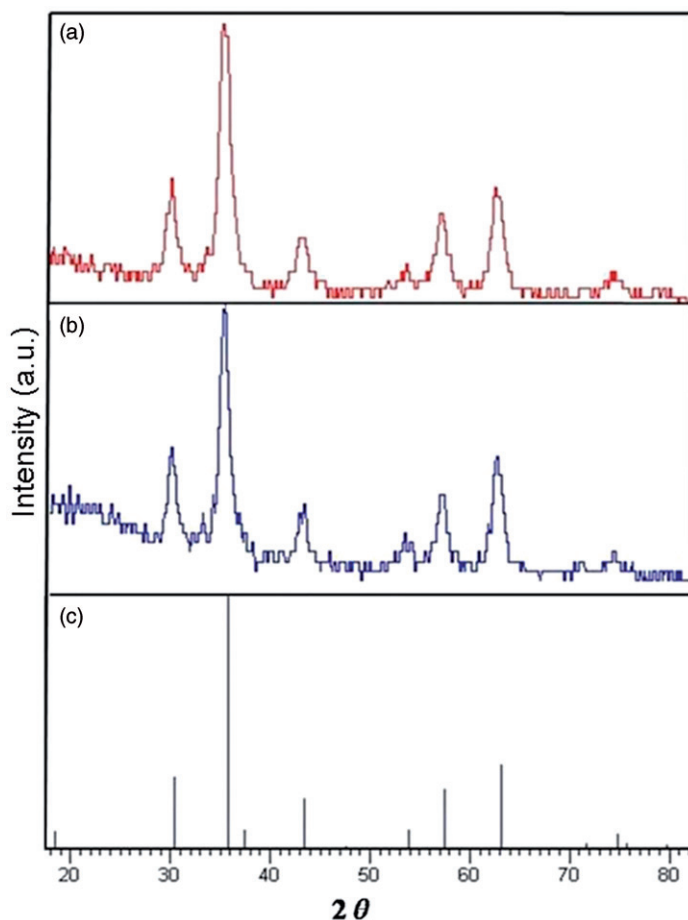
Figure 5. XRD patterns of (a) 350 g/mol mPEG–magnetite complex, (b) 750 g/mol mPEG–magnetite complex and (c) an XRD pattern from the standard Fe_3O_4 powder diffraction data (ICSD no. 01-075-0449).

43.3°, 53.7°, 57.2° and 62.7°) obtained from the standard Fe_3O_4 powder diffraction data (Figure 5). According to the Debye–Scherrer equation, the approximate particle sizes of 350 g/mol mPEG–magnetite complex and 750 g/mol mPEG–magnetite complex were 7.7 and 6.6 nm, respectively. These values are comparable to those determined from TEM analyses. According to VSM analyses, these particles showed superparamagnetic behaviour as indicated by the absence of magnetic remanence and coercitivity (Figure 6). In addition, they exhibited saturation magnetisation (M_s) about 47 and 35 emu/g magnetite, respectively. The higher M_s in the 350 g/mol mPEG–magnetite complex than the other one was attributed to their larger particle sizes, which in turn influenced their magnetic properties.

Stability of particles in water is a major concern if they are anticipated for use in medical application. Hence, the concentrations of magnetite nanoparticles that were stable
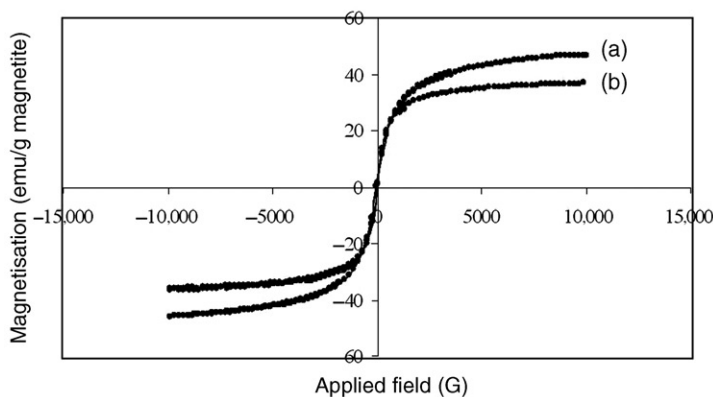
Figure 6. Hysteresis curves of (a) 350 g/mol mPEG–magnetite complex and (b) 750 g/mol mPEG–magnetite complex.

and well dispersible in aqueous dispersions were investigated as a function of time. The dispersions were centrifuged once a week to precipitate unstable particles or large aggregate that may arise and the percentage of Fe_3O_4 in the supernatant was analysed via AAS technique. The initial concentrations of magnetite in water were about 0.2% wt/v for 350 g/mol mPEG–magnetite complex and 0.1% wt/v for 750 g/mol mPEG–magnetite complex. Percentages of stable, dispersible magnetite in aqueous supernatant at each time interval were compared to their initial magnetite concentrations. It was found that the dispersions were stable in aqueous dispersions with insignificant aggregation after 6 weeks of preparing (Table 1). This indicated that these stable magnetite dispersions might be suitable for long-term applications.

Cytotoxicity testing was also performed to investigate their feasible uses in medical applications. The mPEG–magnetite complexes were dried with freeze-drying technique and sequentially diluted with water to obtain various concentrations with maximum concentration up to 50 µg/ml. Cytotoxicity testing was performed against Vero cells via sulforhodamine (SRB) assay method using 0.5% dimethylsulfoxide (DMSO) negative control [30]. The results indicated that the samples were not toxic to vero cells with the concentrations up to 50 µg/ml (supplementary data).

4. Conclusions

Water-dispersible superparamagnetic magnetites were synthesised by thermal decomposition of $Fe(acac)_3$ in mPEG oligomers having $\overline{M}_n$ 350 or 750 g/mol. The use of merely the iron precursor and mPEG oligomers made the reactions easy to scale-up for mass production. FTIR evidenced the existence of hydrophilic mPEG in the complexes, which consequently promoted their long-term stability and dispersibility in water. From TEM result, the particle size of 350 g/mol mPEG–magnetite complex was about 7.8 ± 1.4 nm in diameter, while those of 750 g/mol mPEG–magnetite complex was 5.3 ± 1.1 nm. The hydrodynamic size of 350 g/mol mPEG–magnetite complex and 750 g/mol mPEG–magnetite complex were 37.1 ± 1.0 nm and 35.1 ± 0.4 nm, respectively.

Table 1. Stability of mPEG–magnetite complexes in water.

	Percentage of Fe_3O_4 dispersible in water after				
	0 Week	1 Week	2 Weeks	3 Weeks	6 Weeks
350 g/mol mPEG	100	99.6	99.5	99.4	99.3
750 g/mol mPEG	100	100	99.8	99.7	96.5

According to the calculation from the Debye–Scherrer equation, the sizes of 350 g/mol mPEG–magnetite complex and 750 g/mol mPEG–magnetite complex were 7.7 and 6.6 nm, respectively. The particles were stable in water with insignificant aggregation after 6 weeks of synthesising. This approach thus offered a facile route to prepare water dispersible, non-toxic magnetite nanoparticles having long-term stability in aqueous dispersions, which is a key requirement for biomedical applications.

Acknowledgements

References

[1] R.E. Rosenswei, *Heating magnetic fluid with alternating magnetic field*, J. Magn. Magn. Mater. 252 (2002), pp. 387–389.

[2] M.A. Morales, P.V. Finotelli, J.A.H. Coaquira, M.H.M. Rocha-Leão, C. Diaz-Aguila, E.M. Baggio-Saitovitch, and A.M. Rossi, In situ *synthesis and magnetic studies of iron oxide nanoparticles in calcium-alginate matrix for biomedical applications*, Mater. Sci. Eng., C 28 (2008), pp. 253–257.

[3] K. Donadel, F.D.V. Marcos, V.T. Fávere, M. Rigoni, N.J. Batistela, and M.C.M. Laranjeira, *Preparation and characterization of hydroxyapatite-coated iron oxide particles by spray-drying technique*, Mater. Sci. Eng., C 28 (2008), pp. 509–514.

[4] M.D. Shultz, J.U. Reveles, S.N. Khanna, and E.E. Carpenter, *Reactive nature of dopamine as a surface functionalization agent in iron oxide nanoparticles*, J. Am. Chem. Soc. 129 (2007), pp. 2482–2487.

[5] Y.W. Jun, Y.M. Huh, J.S. Choi, J.H. Lee, H.T. Song, S. Kim, S. Yoon, K.S. Kim, J.S. Shin, J.S. Suh, and J. Cheon, *Nanoscale size effect of magnetic nanocrystals and their utilization for cancer diagnosis via magnetic resonance imaging*, J. Am. Chem. Soc. 127 (2005), pp. 5732–5733.

[6] J. Xiaojun, S. Ruping, A.M. Elliott, R.J. Stafford, E. Esparza-Coss, J.A. Bankson, G. Liang, Z.P. Luo, P. Keeseong, J.T. Markert, and L. Chun, *Bifunctional gold nanoshells with a superparamagnetic iron oxide-silica core suitable for both MR imaging and photothermal therapy*, J. Phys. Chem. C 111 (2007), pp. 6245–6251.

[7] J.H. Choi, F.T. Nguyen, P.W. Barone, D.A. Heller, A.E. Moll, P. Dhaval, S.A. Boppart, and M.S. Strano, *Multimodal biomedical imaging with asymmetric single-walled carbon nanotube/iron oxide nanoparticle complexes*, Nano Lett. 7 (2007), pp. 861–867.

[8] T.K. Jain, M.K. Reddy, M.A. Morales, L. Diandra, L. Pelecky, and V. Labhasetwar, *Biodistribution, clearance, and biocompatibility of iron oxide magnetic nanoparticles in rats*, Mol. Pharmaceutics 5 (2008), pp. 316–327.

[9] M. Aslam, E.A. Schultz, T. Sun, T. Meade, and V.P. Dravid, *Synthesis of amine-stabilized aqueous colloidal iron oxide nanoparticles*, Cryst. Growth Des. 7 (2007), pp. 471–475.

[10] K.E. Hee, A. Yangkyu, and L.H. Sook, *Biomedical applications of superparamagnetic iron oxide nanoparticles encapsulated within chitosan*, J. Alloys Compd. 434 (2007), pp. 633–636.

[11] M.V. Yigit, D. Mazumdar, and Y. Lu, *MRI detection of thrombin with aptamer functionalize superparamagnetic iron oxide nanoparticles*, Bioconjugate Chem. 19 (2008), pp. 412–417.

[12] P. Daksha, J.Y. Moon, C. Yongmin, K.T. Jeong, and L.G. Ho, *Poly(D,L-lactide-co-glycolide) coated superparamagnetic iron oxide nanoparticles: Synthesis, characterization and* in vivo *study as MRI contrast agent*, Colloids Surf., A 313 (2008), pp. 91–94.

[13] S. Mohapatra, S.K. Mallick, T.K. Maiti, S.K. Ghosh, and P. Pramanik, *Synthesis of highly stable folic acid conjugated magnetite nanoparticles for targeting cancer cells*, Nanotechnology 18 (2007), p. 385102.

[14] M. Babic, D. Horák, M. Trchová, P. Jendelová, K. Glogarová, P. Lesný, V. Herynek, M. Hájek, and E. Syková, *Poly(L-lysine)-modified iron oxide nanoparticles for stem cell labeling*, Bioconjugate Chem. 19 (2008), pp. 740–750.

[15] Y. Chengli, A. Rait, K.F. Pirollo, J.A. Dagata, N. Farkas, and E.H. Chang, *Nanoimmunoliposome delivery of superparamagnetic iron oxide markedly enhances targeting and uptake in human cancer cells* in vitro *and* in vivo, Nanomed. Nanotechnol. Biol. Med. 4 (2008), pp. 318–329.

[16] T.K. Jain, M.K. Reddy, M.A. Morales, L. Diandra, L. Pelecky, and V. Labhasetwar, *Iron oxide nanoparticles for sustained delivery of anticancer agents*, Mol. Pharmaceutics 2 (2005), pp. 194–205.

[17] P.S. Haddad, T.M. Martins, L. D'Souza-Li, L.M. Li, K. Metze, R.L. Adam, M. Knobel, and D. Zanchet, *Structural and morphological investigation of magnetic nanoparticles based on iron oxides for biomedical applications*, Mater. Sci. Eng., C 28 (2008), pp. 489–494.

[18] N. Pinna, S. Grancharov, P. Beato, P. Bonville, M. Antonietti, and M. Niederberger, *Magnetite nanocrystals: Nonaqueous synthesis, characterization, and solubility*, Chem. Mater. 17 (2005), pp. 3044–3049.

[19] C. Wei and J. Wan, *Facile synthesis of superparamagnetic magnetite nanoparticles in liquid polyols*, J. Colloid Interface Sci. 305 (2007), pp. 366–370.

[20] Z. Li, H. Chen, H. Bao, and M. Gao, *One-pot reaction to synthesize water-soluble magnetite nanocrystals*, Chem. Mater. 16 (2004), pp. 1391–1394.

[21] J.F. Lutz, S. Stiller, A. Hoth, L. Kaufner, U. Pison, and R. Cartier, *One-pot synthesis of PEGylated ultrasmall iron-oxide nanoparticles and their* in vivo *evaluation as magnetic resonance imaging contrast agents*, Biomacromolecules 7 (2006), pp. 3132–3138.

[22] S. Chairam and E. Somsook, *Starch vermicelli template for synthesis of magnetic iron oxide nanoclusters*, J. Magn. Magn. Mater. 320 (2008), pp. 2039–2043.

[23] H. Lee, M.K. Yu, P. Sangjin, M. Sungmin, J.J. Min, Y.Y. Jeong, K. Hae-Won, and J. Sangyong, *Thermally cross-linked superparamagnetic iron oxide nanoparticles: Synthesis and application as a dual imaging probe for cancer* in vivo, J. Am. Chem. Soc. 129 (2007), pp. 12739–12745.

[24] G. Shuyan, S. Youguo, Z. Shuxia, J. Kai, Y. Shuxia, L. Zhengdao, and E.T. Muromachi, *Biopolymer-assisted green synthesis of iron oxide nanoparticles and their magnetic properties*, J. Phys. Chem., C 112 (2008), pp. 10398–10401.

[25] J. Zhang, S. Xu, and E. Kumacheva, *Polymer microgels: Reactors for semiconductor, metal, and magnetic nanoparticles*, J. Am. Chem. Soc. 126 (2004), pp. 7908–7914.

[26] P. Dallas, V. Georgakilas, D. Niarchos, P. Komninou, T. Kehagias, and D. Petridis, *Synthesis, characterization and thermal properties of polymer/magnetite nanocomposites*, Nanotechnology 17 (2006), pp. 2046–2053.

[27] K.J. Sreeram, I. Ramasamy, R. Ananthanarayanan, B.U. Nair, and R. Thirumalachari, *Template synthesis of highly crystalline and monodisperse iron oxide pigments of nanosize*, Mater. Res. Bull. 41 (2006), pp. 1875–1881.

[28] T. Theppaleak, G. Tumcharern, U. Wichai, and M. Rutnakornpituk, *Synthesis of water dispersible magnetite nanoparticles in the presence of hydrophilic polymers*, Polym. Bull. 63 (2009), pp. 79–90.

[29] O. Bomat-Miguel, P. Tartaj, M.P. Morales, P. Bonville, U. Golla-Schindler, X.Q. Zhao, and S. Veintemillas-Verdaguer, *Core-shell iron-iron oxide nanoparticles synthesized by laser-induced pyrolysis*, Small 2 (2006), pp. 1476–1483.

[30] V. Vichai and K. Kirtikara, *Sulforhodamine B colorimetric assay for cytotoxicity screening*, Nat. Protoc. 1 (2006), pp. 1112–1116.